IPPI
Polyolefins Journal, Vol. 6, No. 2 (2019)
DOI: 10.22063/poj.2019.2295.1123

ORIGINAL PAPER

Thermal behavior of ethylene/1-octene copolymer fractions at high temperatures: Effect of hexyl branch content

Abbas Kebritchi*[1], Mehdi Nekoomanesh[1], Fereidoon Mohammadi[1], Hossein Ali Khonakdar[1], Udo Wagenknecht[2]

[1]Iran Polymer and Petrochemical Institute, 14965-115, Tehran, Iran

[2]Leibniz-Institut für Polymerforschung Dresden e.V., D-01069, Dresden, Germany

Received: 6 September 2018, Accepted: 25 February 2019

ABSTRACT

In this work, the effect of hexyl branch content on thermal behavior of a fractionated ethylene/1-octene copolymer with emphasis on high temperatures was investigated. The ethylene/1-octene copolymer was carefully fractionated to different fractions with homogenous hexyl branch (HB) content by preparative temperature rising elution fractionation (P-TREF) method. The P-TREF fractions were thermally analyzed via differential scanning calorimetry (DSC), thermogravimetric analysis (TGA) and evolved gas analysis (EGA). The P-TREF profile showed a short chain branch distribution (SCBD) of around 1.24. A linear relationship between P-TREF elution temperature (ET) and methylene sequence length (MSL) was presented. The DSC curves exhibited a monolithically increase in melting temperature (T_m) as well as crystallization temperature (T_c) with decreasing short chain branch (SCB) content. The calculated values of lamellae thickness suggested a linear function of SCB content and T_m. The TGA studies of P-TREF fractions depicted a two-stage thermal degradation behavior: pre-degradation and main degradation stages. T_{max} for both pre-degradation and main degradation stages increased for fractions with less hexyl branch content. As an interesting point the pre-degradation stage was more intensified for more linear fractions. The concentration of main products was found to be affected by the content of hexyl branches using Py-GC-MS. **Polyolefins J (2019) 6: 127-138**

Keywords: Thermal behavior; ethylene/1-octene copolymer; hexyl branch content; thermal degradation.

INTRODUCTION

During the last 50 years, polymer science has advanced rapidly because of the major breakthroughs on polymer structure, properties and usage [1,2]. Polyethylene (PE) is the largest volume synthetic polymer in the world [3,4]. Linear low-density polyethylene (LLDPE) (copolymer of ethylene and α-olefin) is a commercially important class of polyethylenes [5-7]. The ethylene copolymers made with solid, supported Ziegler–Natta (Z-N) catalysts are mixtures of chains that have different amounts of comonomer [3,8]. In contrast to the broad comonomer and molecular weight distributions of LLDPEs synthesized with multisite catalysts, the metallocene-based copolymers have narrow molecular weight distribution and homogeneous inter- and intra-

* Corresponding Author - E-mail: a.kebritchi@ippi.ac.ir

molecular distribution of comonomer units [9-11].

Copolymers of ethylene and α-olefin resins with homogeneous branching distribution behave as elastomers at high short-chain branching levels and act as typical thermoplastics at low short-chain branching levels [12]. Bensason et al. have examined the deformation of low-crystallinity ethylene-octene copolymers in uniaxial tension as a function of comonomer content and molecular weight [9]. Bensason et al. have also reported mechanical behavior of ethylene-octene copolymer prepared by Dow's INSITETM constrained geometry catalyst technology (CGCT). They showed that as the comonomer content increases (from 2.8 to 13.6 mole%), the accompanying tensile behavior changes from necking and cold drawing in typical of a semicrystalline thermoplastic to uniform drawing and high recovery characteristic of an elastomer [13]. Brady and Thomas have worked on DSC characterization of LLDPE samples with approximately equal average branch content and different α-olefin types (1-betene, 1-hexene and 1-octene) revealed that, the α-transition temperature shifts to lower temperatures as branch content increases [14]. Mileva et al. have studied the role of crystallinity and crystal habit in tensile properties of ethylene copolymers [15].

It is well established that copolymer properties depend on the type, amount, and distribution of comonomer [3,16-19]. In ethylene-1-alkene copolymers every incorporation of a 1-alkene or α-olefin comonomer unit introduces a short chain branch in the polymer chain causing a disruption of the chain regularity [20]. It is noted that, the short chain branches (SCBs) in homogeneous ethylene copolymers have a predominant effect on crystallization and melting behaviors [21,22]. It is known that the crystallizability is affected by molecular weight, concentration of branches, and their distribution along the copolymer backbone [5]. Alamo and Mandelkern have reviewed the dependency of crystallization and melting parameters on comonomer content for different ethylene/α-olefin copolymers [23]. Zhang et al. have investigated the roles of the branch content and branch type in the copolymer crystallization by molecular dynamic (MD) simulations for two series of single copolymer chain models with precisely controlled methyl branching and with branches of different lengths. They showed that the branch content plays an important role in determining whether a single chain can form a lamellar structure or not. With the decreasing of the branch contents, more perfect lamellar structure is formed and the crystallinity of the polymer increases. Also they found that the branch point is always rejected to the folded surface of the lamellar structure as a defect, and the critical chain length for side-chain crystallization is 10 carbons [5]. Experimentally it is obtained that hexyl branches are not incorporated in the crystal lattice. Longer branches will not be incorporated, but side chain crystallization of the branches might occur [20]. It has been known that the melting temperatures of ethylene/α-olefin copolymers may vary by 10s of degrees Celsius when the comonomer type and overall amount are the same, suggesting the importance of comonomer distribution [3]. Ethylene copolymerization with fairly bulky α-olefin monomers like 1-octene results in hexyl branches that are excluded from the crystals, lowering the crystallinity and hence the physical density [10]. Most of the works have concentrated on the role of branching in low-temperature thermal behavior of ethylene/α-olefin copolymers, but the question rises what is branching role in high-temperature thermal behavior or thermal degradation?

In our previous works the effect of molecular weight on thermal degradation of polyolefins [24] as well as effect of ethyl and butyl branch content [25-28] on thermal and catalytic degradation was investigated in depth. In this study the effect of hexyl branch content on thermal degradation of ethylene/1-octene copolymer based on metallocene catalyst is examined which are usually ignored. To study accurately and to eliminate any other microstructural parameters; the ethylene/1-octene copolymer was fractionated to homogenous SCB content fractions using P-TREF technique which separates fractions based on SCB content only at low cooling rates not the molecular weight [29-31]. The role of SCB content on crystallization, melting, thermal degradation (P-TREF/TGA technique) and Py-GC-MS of each fraction is investigated in order to establish a correlation between low and high thermal behavior and the comonomer content of metallocene-based ethylene/1-octene copolymer.

EXPERIMENTAL

Material

"Parent polymer" was an ethylene/1-octene copolymer laboratory synthesized based on metallocene catalyst (Table 1). Molecular weight and polydispersity of parent LLDPE as well as P-TREF fractions were evaluated using a high-temperature size exclusion chromatography (SEC) apparatus PL-GPC 220 (Polymer Laboratories) at 150°C coupled with a multi-angle laser light scattering (MALLS) (Helleos II, Wyatt Technology Corp., USA) and a RI detector. The column set was two SEC columns 300×7.5 mm PLgel-Olexis. The eluent was 1,2,4-trichlorobenzene (TCB, Merck) stabilized with 0.02 wt% 2,6-di-tert-butyl-p-cresol (BHT) used with flow velocity of 1.0 ml/min (Figure 1). By considering of Figure 1 and Figure 2 a narrow molecular weight and short chain branch distribution type for the parent polymer can be concluded. Hexyl content of the parent polymer was calculated based on hydrogen-1 nuclear magnetic resonance (^{1}H NMR) and presented in Table 1.

Preparative temperature rising elution fractionation (P-TREF)

The home-made P-TREF consisted of a cylindrical column 7 cm in diameter and 40 cm in height. This column was packed by seeds with average diameter of 0.07 cm and submerged in an oil bath with a programmable thermostat that controlled the temperature of the bath. In each run a polymer solution with concentration of 1 wt.% of parent polymer in xylene was introduced into the column and heated at 140°C for 2 h and then, cooled to room temperature (30°C) slowly at a rate of -3 °C/h in order to crystallize the polymer on the seeds. The cooling rate is as slow as that the fractions are only separated base on SCB content not the molecular weight [25-27]. The bath temperature was subsequently increased and maintained for about 2 h at each fraction temperature to elute polymer chains of specific crystallizability completely by a stream of pure solvent (xylene). After dissolution of polymer chains, the fractions in solvent stream were treated with anti-solvent (acetone) to separate the polymer fractions. After separation, the prepared fractions were tested by subsequent thermal analysis including DSC, TGA, headspace-GC-MS and pyrolysis-GC-MS.

Table 1. Specifications of the parent polymer

Property	Test method	Typical value
Melting point (°C)	ISO 3146	117.97
Melt flow index (MFI) (190°C/2.16 Kg) (g/10 min)	ISO 1133	1.96 ± 0.07
Melt flow index (MFI) (190°C/21.6 Kg) (g/10 min)	ISO 1133	70.71 ± 1.21
Molecular weight (M_w)	-	96,000
Molecular weight (M_n)	-	21,000
Polydispersity index (PDI)	-	4.50
Hexyl content (mol%)	^{1}H NMR	2.99

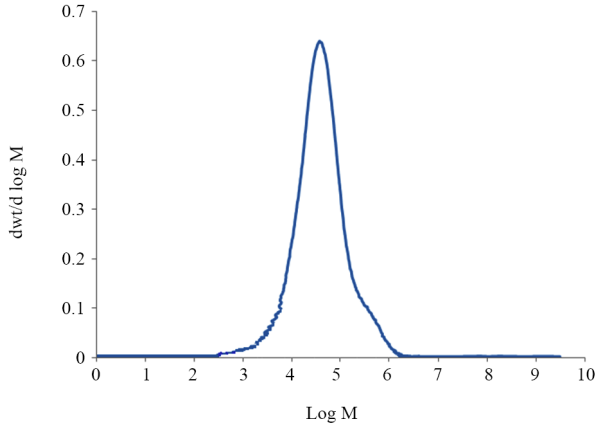

Figure 1. Molecular weight distribution of the parent copolymer

Differential scanning calorimetry (DSC)

Thermograms of different fractions were assessed by a Mettler differential scanning calorimetry (Toledo, Switzerland) under N_2 atmosphere, in which the samples were heated fast (200°C/min) to 180°C and maintained at this temperature for 5 min to erase any thermal history, and then cooled to room temperature (30°C) at a rate of -10°C/min. This was immediately followed by a second heating run (10°C/min) in order to detect a complete melting behavior of the samples.

Thermogravimetric analysis (TGA) and derivative thermogravimetry (DTG)

The thermogravimetric analysis of different fractions was made using TGA Q 5000 of TA Instruments, under N_2 purge at 20 ml/min. The fractions experienced an isothermal condition for 5 min at room temperature and then heated up with a ramp at 10, 25, 50 and 100°C/min to 600°C. The samples were powder the with weight of about 10^{-13} mg.

Pyrolysis-gas chromatography-mass spectrometery (Pyrolysis-GC-MS)

A Pyroprobe pyrolyzer (5000 v. CDS Analytical, Inc., USA) was employed with platinum filament and interface CDS1500 at 250°C. The pyrolysis was based on step-wise at determined temperatures for different fractions and the pyrolysis time was 10 s for each temperature step; characterized by an Agilent Technologies GC (7890 A v) with inlet-temperature of 280°C, GC-oven temperature of 2 min at 50°C; then 12°C/min to 280°C and 10 min at 280°C. GC-column was HP-5MS (non-polar); 30 m × 250 μm ID (inner diameter) × 0.25 μm SD (layer thickness) and carrier gas was helium 1 ml/min. MSD (mass selective detector) 5975C inert XL EI/CI EI at 70 eV with mass scan range of 15-550.

Structural characterization

FTIR spectrometer (Vertex 80, Bruker, Germany) was used to characterize the parent polymer structure. The ATR spectra were recorded in the range of 4000–600 cm^{-1}, 100 scans each measurement with resolution of 2 cm^{-1} using an MCT detector. The ^{1}H NMR spectra were recorded on a Bruker DRX 500 spectrometer operating at 500.13 MHz. C2D2Cl4 was employed as the solvent at 120°C. The spectra were referenced on the residual C2HDCl4 signal δ(1H) = 5.98 ppm.

RESULTS AND DISCUSSION

Investigation on the short chain branch distribution (SCBD)

Figure 2 represents the P-TREF profile of parent polymer. A narrow short chain branch distribution (SCBD) for the parent polymer can be acquired from Figure 2, which can be attributed to the metallocene type of catalyst used for polymer synthesis. It is well known that the molecular structure can be controlled by the catalyst [32] as well as metallocene catalysts with the single-site character of the active species [33] allow a perfect control over the chain microstructure [34] and generates polymers with narrow, monomodal Flory-size distributions [33].

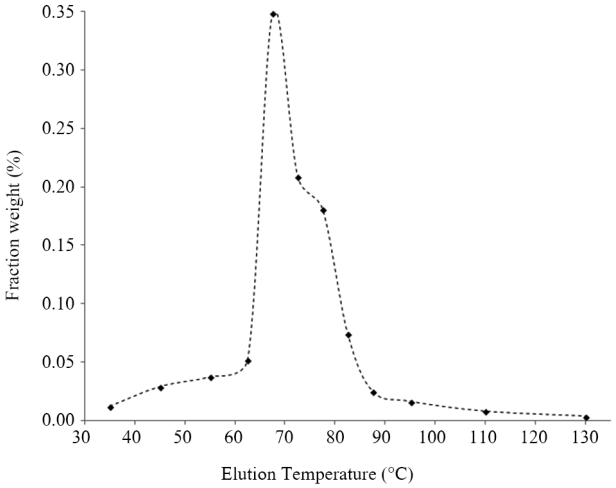

Figure 2. P-TREF profile of the parent polymer.

Relationships of hexyl branch content with crystallization and melting behavior

DSC thermograms of the second heating cycle and the melting temperatures of P-TREF fractions are presented in Figure 3, while the detailed information is tabulated in Table 2. Due to small amount of some fractions, acquired at 30-40°C, 40-50°C, 50-60°C, 60-65°C, 85-90°C, 90-100°C, 100-120°C and 120-140°C, the thermal analysis of the samples is limited to the fractions mentioned in Table 2. In Figure 3, a fine confirmation on distinctive separation of P-TREF fractions can be detected as complete segregated melting peaks are observed.

Zhang and Wanke showed that MSL as a function of the melting temperature (T_m) in °K can be estimated by a calibration correlation [35], using Equation 1:

$$MSL = \frac{2}{\exp\left(\frac{142.2}{T_m} - 0.3451\right) - 1} \quad (1)$$

In Figure 4, the variation of methylene sequence length (MSL) against elution temperature (ET) is plotted. As it can be observed from Figure 4 the MSL is increased by elution temperature through a linear function predicted by Equation 2:

$$MSL = 24.9\, e^{0.02\,(ET)} \quad (2)$$

The exponential function for increase of MSL versus ET is confirmed for ethylene/α-olefin copolymers in the literature through increasing ethylene content [36]

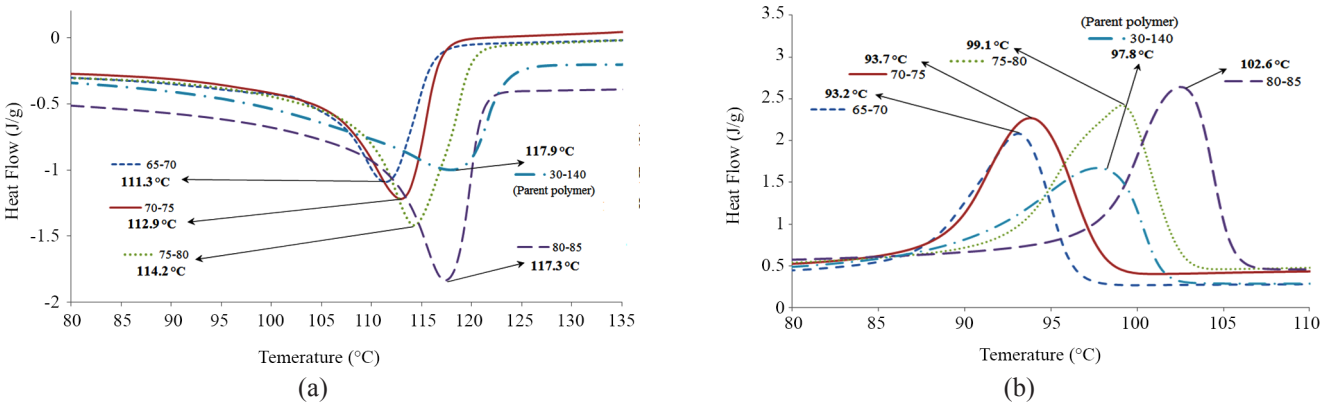

Figure 3. DSC curves at second heating mode with melting temperatures (left) and cooling mode with crystallization temperatures (right), for different ethylene/1-octene fractions.

and decreasing short chain branch content [37] by elution temperature.

By counting the carbon atoms and CH_3 groups for the 'repeating unit' in an ethylene/α-olefin molecule with the same methylene sequence length and neglecting the effect of end groups, the short chain branch content, SCB, per 1000 carbons, as a function of MSL can be estimated by Equation 3 [35], where i is the carbon number in the branch (e.g., for 1-octene comonomer, i is equal to 6).

$$SCB = \frac{1000}{MSL + i + 1} \quad (3)$$

The number average short chain branch content, $\overline{SCB_n}$, and weight average short chain branch content, $\overline{SCB_w}$, can be calculated based on the first and second moments of the SCB distributions, similar to the number and weight average molecular weight distributions, according to Equations 4 and 5:

$$\overline{SCB_n} = \sum_{i=1}^{n} w_i \times SCB_i \quad (4)$$

$$\overline{SCB_w} = \frac{\sum_{i=1}^{n} w_i \times SCB_i^2}{\sum_{i=1}^{n} w_i \times SCB_i} \quad (5)$$

Where wi is the mass fraction of fraction i (obtained from P-TREF results), SCB_i is the SCB content of fraction i (calculated based on Equation 3) and n is the number of fractions (here n=4). Using Equations 4 and 5, $\overline{SCB_n}$ and $\overline{SCB_W}$ were calculated 8.826 and 10.911, respectively. Also in a similar way for calculation of MWD, the SCBD can be calculated using Equation 6:

$$SCBD = \frac{\overline{SCB_w}}{\overline{SCB_n}} \quad (6)$$

The amount of SCBD was calculated around 1.24. In comparison to the literature [35, 38], the obtained SCBD value can be assumed as a broad SCBD. According to the Gibbs–Thomson relationship (Equation 7), it is possible to determine the lamellae thickness (Lc) of different lamellaes [39]:

$$T_m = T_m^0 - \frac{1 - 2\delta_c}{\Delta H \times L_c} \quad (7)$$

Where T_m (°K) is the observed melting point, Tom (°K) is the equilibrium melting point of an infinite polyethylene crystal (414.5 °K), ΔH is the enthalpy

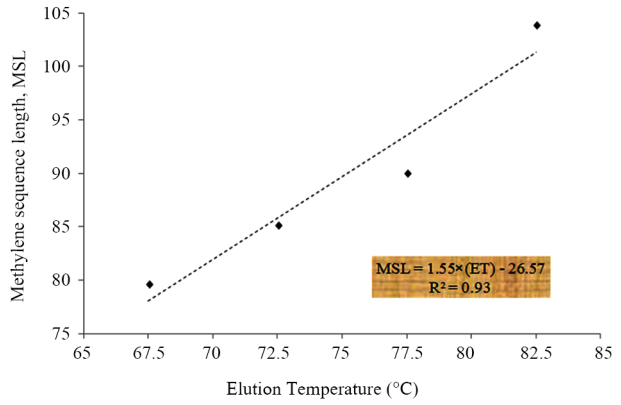

Figure 4. MSL variations of the fractions versus elution temperature.

Table 2. Detailed DSC data and the calculated parameters of P-TREF fractions.

Fraction	Weight (g)	Melting onset temperature (°C)	Crystallization onset temperature (°C)	SCB[(1)] (br/1000 C)	L_c[(2)] (nm)	X_c[(3)] (%)	MSL[(4)]
65-70	0.829	103.7	96.3	11.5	6.7	29.2	79.7
70-75	0.497	103.9	98.1	10.9	7.1	30.7	85.2
75-80	0.430	107.2	102.5	10.3	7.4	36.7	90.0
80-85	0.177	110.1	105.6	9.0	8.4	36.2	103.9
30-140 (Parent polymer)	2.378	98.4	101.5	8.8	8.6	34.0	107.3

[(1)]SCB: Short chain branch content calculated by Equation 3.
[(2)]Lc: Lamellae thickness calculated by Gibbs-Thomson relationship (Equation 7).
[(3)]X_c: Crystallinity calculated by Equation 8.
[(4)]MSL: Methylene sequence length calculated by Equation 1.

of fusion per unit volume (288×106 J/m^3), δ_c is the surface energy of a polyethylene crystal (70×10^{-3} J/m^2) and L_c (nm) is the thickness of a lamellae with melting point of T_m [40]. Also the crystallinity of each fraction can be calculated using Equation 8:

$$T_C(\%) = \frac{\Delta H_f}{\Delta H_f^0} \times 100 \quad (8)$$

Where ΔH_f is the enthalpy of fusion of each fraction and ΔH_f° is the enthalpy of fusion of 100% crystalline polyethylene (286 J/g) [41].

In Figure 5, melting and crystallization temperatures are plotted against short chain branch content. Based on these observations, linear Equations 9 and 10 are proposed, respectively, for predicting the reduction of T_m versus SCB and estimating the decrease of T_c against SCB.

$$T_m = -2.4\times(SCB)+138.9 \quad (9)$$

$$T_c = -4.0\times(SCB)+139.3 \quad (10)$$

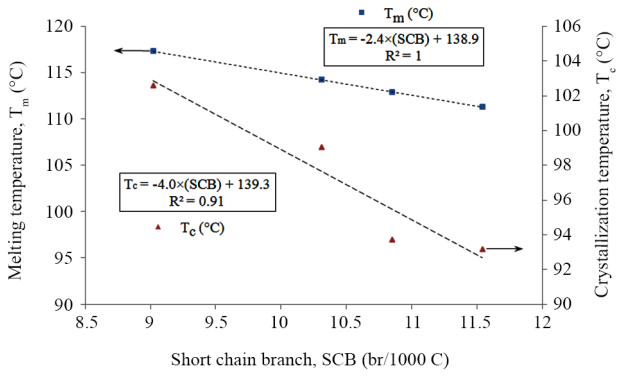

Figure 5. Variations of melting and crystallization temperatures versus short chain branch for P-TREF fractions

As it is acquired from the comparison of Equations 9 and 10, the crystallization temperature (T_c) is more sensitive to SCB content than melting temperature, because the magnitude of slope in Equation 10 is about 1.7 times larger than the slope in Equation 9. Equation 9 is analogous to equation $T_m = -2.55\times(SCB)+132.54$, proposed by Wiflong and Knight for P-TREF fractions of a metallocene-based ethylene-1-octene copolymer [42]. But in comparison with equation $T_m = -2.176\times(SCB)+132.18$, proposed by the same authors for P-TREF fractions of a Zeiegler-Natta (Z-N)-based ethylene-1-octene copolymer, small variations can be observed especially at SCB coefficient. This difference may be attributed to the differences in type of the catalysts. As M. Zhang et al. showed the type of catalyst has a substantial effect on the coefficient of SCB [43].

Figure 6 shows the changes of SCB content and melting temperature versus lamellae thickness. As it can be observed in Figure 6, the SCB content is reduced through a linear correlation predicted by Equation 11 by L_c. Also by increasing the lamellae thickness the melting temperature is increased again by a linear

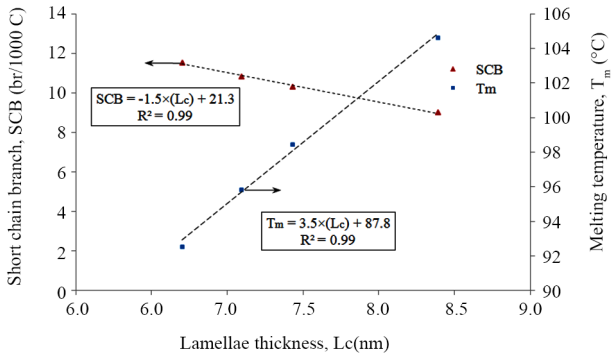

Figure 6. Variations of short chain branch content and melting temperature against lamellae thickness for P-TREF fractions.

relationship predicted by Equation 12. By comparison of Equations 12 and 9 it can be concluded that T_m is more sensitive to lamellae thickness than short chain branch content, as the magnitude of coefficient for SCB in Equation 9 is smaller than the magnitude of coefficient Lc in Equation 12.

$$SCB = -1.5 \times (L_c) + 21.3 \quad (11)$$

$$T_m = 3.5 \times (L_c) + 87.8 \quad (12)$$

The interesting point is that for prediction of SCB changes against L_c for P-TREF fractions of both metallocene- and Ziegler-Natta-based ethylene-1-butene copolymers, exponential relationships are reported in the literature, e.g., $L_c = 7.14 \times \exp(-0.021 \times SCB)$ for metallocene [43] and $L_c = 20.482 \times \exp(-0.038 \times SCB)$ for Ziegler-Natta [44]. This may be originated from the low range of SCB content that is studied here. Because we have observed an exponential function, $L_c = 28.39 \times \exp(-0.129 \times SCB)$ for Phillips-based ethylene/1-hexene copolymer P-TREF fractions, in our previous work [45]. Therefore, it may be concluded that at low SCB contents the L_c is a linear function of SCB but at higher SCB contents it shows an exponential correlation.

Correlation between hexyl branch content and thermal degradation parameters

TGA/differential thermogravimetric (DTG) analysis was carried out on the parent polymer and its P-TREF fractions. The thermogravimetric data are provided in Table 3 and TGA/DTG curves are depicted in Figure 7. As it can be seen in Figure 7, a pre-degradation occurs at temperature range of about 352 to 357°C for fractions of 70-75, 75-80 and 80-85. The temperature at maximum degradation rate in pre-degradation stage is called hereafter as "pre-T_{max}". Pre-T_{max} is increased for these fractions by decreasing short chain branch content. The amount of mass loss at the Pre-T_{max} is also increased by decreasing SCB content.

Due to the existence of the pre-degradation it seems to be impossible to calculate the accurate amount of degradation initiation temperature ($T_{5\%}$) for these fractions. Therefore, $T_{5\%}$ is not reported in Table 3 for these fractions. Considering the variations of T_{max} vs SCB content in Table 3, it can be seen that an initial increase in the amount of T_{max} from about 469°C to around 478°C is occurred by decreasing SCB content from 11.54 to 10.85 (br/1000 C). After this jump, approximately constant values for T_{max} can be observed even at lower SCB contents up to 9.02 (br/1000 C).

Effect of hexyl branch content on pyrolysis products

To evaluating the effect of hexyl branch content on the degradation products, pyrolysis-GC-MS was carried out on different P-TREF fractions at three important stages of thermal degradation which are degradation initiation temperature ($T_{5\%}$), temperature at maximum degradation rate (T_{max}) and degradation termination temperature ($T_{95\%}$). The test was a stepwise pyrolysis-GC-MS which samples were maintained at each temperature step for about 10 s. The obtained chromatograms in each temperature step have been plotted in Figures 8-10. As it can be observed in Figures 8-10, a 3-D representation of pyrolysis-GC-MS chromatograms for each temperature is plotted which shows relative intensity of evolved gases against

Table 3. TGA/DTG data of the parent polymer and the P-TREF fractions.

Fraction	$T_{5\%}$ [(1)] (°C)	$T_{95\%}$ [(2)] (°C)	T_{max} of pre-degradation [(3)] (°C)	Mass loss at pre-degradation (%)	T_{max} of main-degradation [(4)] (°C)	SCB [(5)] (br/1000 C)
65-70	432.3	487.5	-	-	469.3	11.5
70-75	-	491.3	352.3	0.6	478.3	10.9
75-80	-	490.2	356.6	1.7	477.2	10.3
80-85	-	490.7	356.9	11.9	477.6	9.0
30-140 (parent polymer)	440.7	493.5	-	-	480.1	8.8

[(1)] $T_{5\%}$: Temperature at 5% mass loss (degradation initiation temperature).
[(2)] $T_{95\%}$: Temperature at 95% mass loss (degradation termination temperature).
[(3)] Temperature at maximum degradation rate in pre-degradation stage.
[(4)] Temperature at maximum degradation rate in main degradation stage.
[(5)] SCB: Short chain branch content.

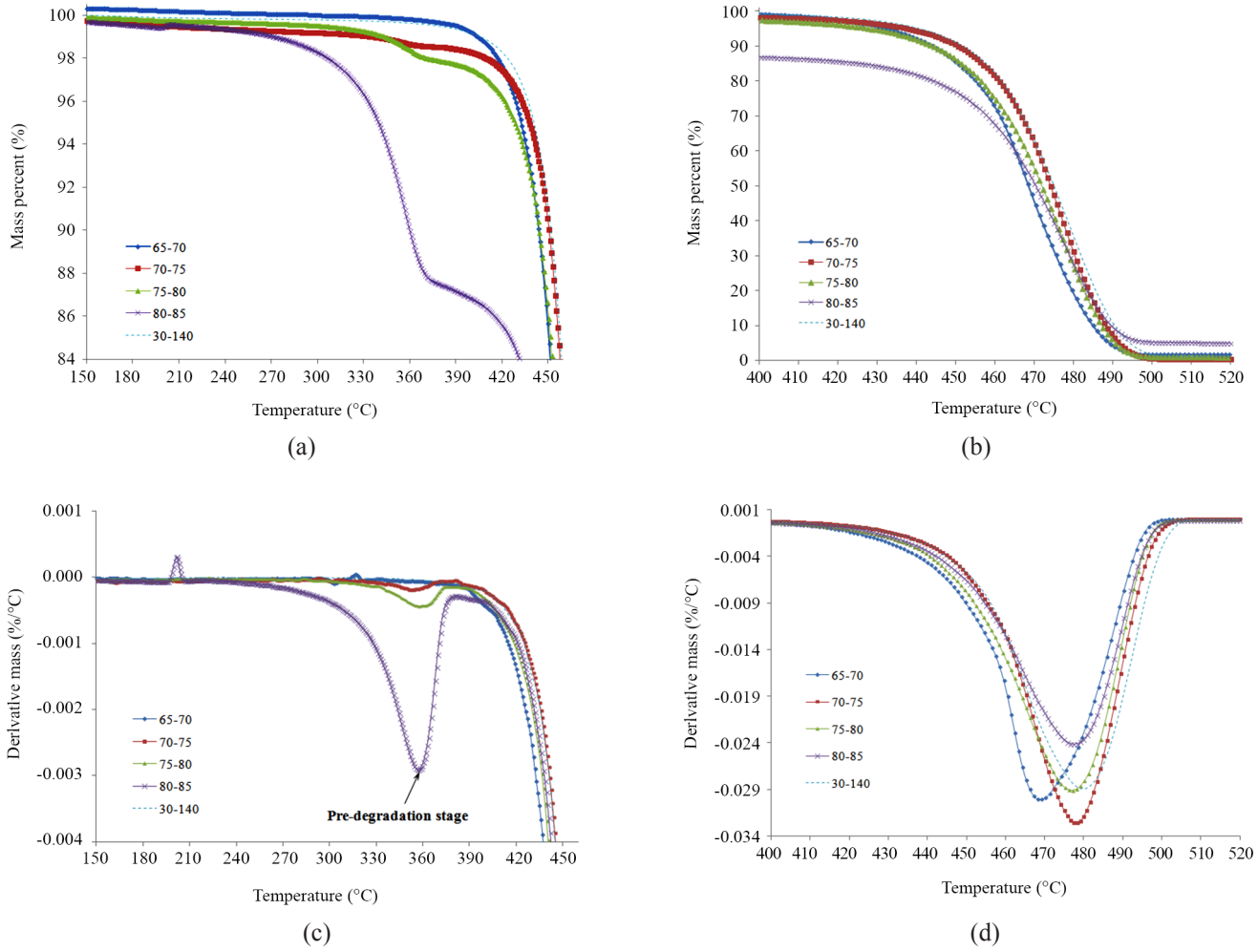

Figure 7. TGA and DTG curves of P-TREF fractions. An adapted expanded scale is used for each fraction for better comparison of degradation peak shapes: (a) TGA curves of initiation stage (150-460°C), (b) TGA curves of propagation stage (400-520°C), (c) DTG curves of initiation stage (150-460°C), (d) DTG curves of propagation stage (400-520°C).

short chain branch content (hexyl branch content) and retention time.

The depth axis shows retention time of evolved gases which is an indication of differences in boiling points through GC column [46]. As the boiling point depends on the molecular weight [47], therefore, depth axis can illustrate molecular weight of evolved gases. The vertical axis shows relative intensity of different peaks which corresponds to relative concentration of each compound [46]. The horizontal axis indicates short chain branch content. As it is noticed in comparison of Figures 8-10, the number of peaks which intonates the

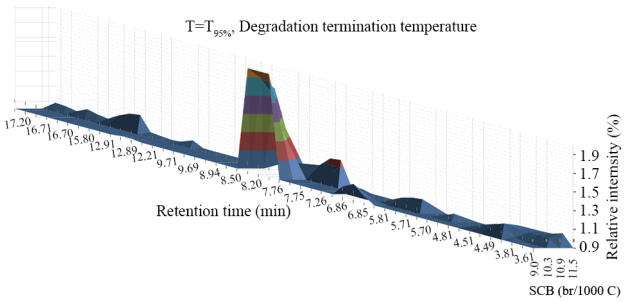

Figure 8. 3-D variations of relative intensity of products of pyrolysis-GC-MS against short chain branch content and retention time at $T_{5\%}$, degradation initiation temperature.

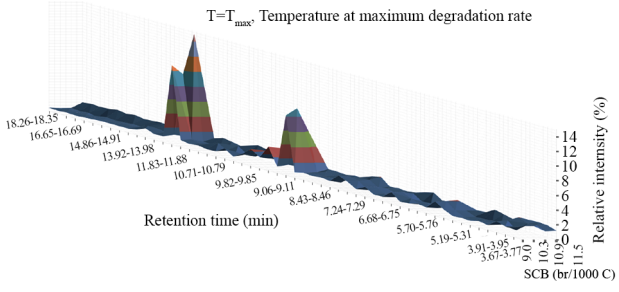

Figure 9. 3-D variations of relative intensity of products of pyrolysis-GC-MS against short chain branch content and retention time at T_{max}, temperature at maximum degradation rate.

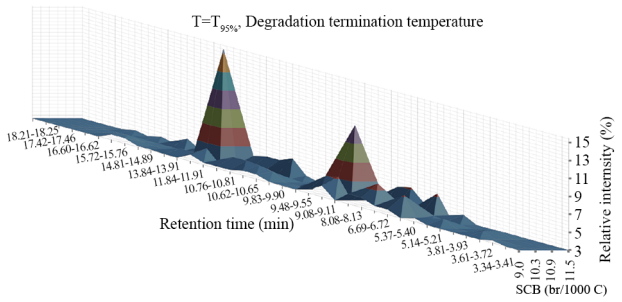

Figure 10. 3-D variations of relative intensity of products of pyrolysis-GC-MS against short chain branch content and retention time at $T_{95\%}$, degradation termination temperature.

number of products [46] is most at the $T_{95\%}$ (Figure 10). This may be attributed to the fact that by increasing the degradation temperature the number of products is increased. The overall thermal decomposition mechanism for PE can be described by free radical processes [48]. As temperature is increased, more scissions in the polymer chain occur leading to a high number of short primary radicals, which undergo successive β-scission reactions and eliminate small molecules [49]. For degradation at $T_{5\%}$ (Figure 8) a main peak is observed from 7.76 to 8.50 min which decreases with SCB content. But, for degradation at T_{max} and $T_{95\%}$ (Figures 9-10) two important peaks are observed which both increase with SCB content. Also by comparison of Figures 8-10 it can be concluded that with increasing temperature, main product (observed from 7.76 to 8.50 min at $T_{5\%}$) shifts to higher molecular weight products (observed from 9.41 to 9.90 min at $T_{95\%}$). Moreover for degradation at $T_{5\%}$ (Figure 8) only one main peak is observed between 7.76 and 8.50 min, although at higher temperatures (T_{max} and $T_{95\%}$) another main peak is observed between 11 and 14 min which can be related to products with higher molecular weights. In other word, the higher radical concentration (at higher temperatures) favors intermolecular hydrogen transfer and increases the bimolecular reaction probability [49]. As β-scission is favored at higher temperatures (≈500°C, near to $T_{95\%}$ of ethylene/1-octene copolymer) [50] and presence of higher SCB leads to more β-scissions (due to tertiary carbon existence), therefore by increasing the temperature and SCB content degradation of ethylene/1-octene copolymer may lead to increase the high molecular weight products (Figures 8-10) which would be mainly alkenes according to the Rice/Kossiakoff mechanism [51].

CONCLUSION

The results obtained in this work have shown that the content of hexyl branch in ethylene/1-octene copolymer plays an important role in thermal behavior. The DSC study has shown that melting temperature as well as crystallization temperature is increased by decreasing hexyl branch content linearly. Also in contrast to ethyl and butyl branch content for ethylene/1-butene and ethylene/1-hexene copolymers, respectively, which show exponential correlations in the literature, lamellae thickness has depicted a linear correlation with hexyl branch content here. Two different degradation peaks have been observed for ethylene/1-octene copolymer fractions at around 350 °C and 470 °C. At higher linear chains the first degradation stage is more intensified. Pyrolysis-GC-MS results have shown that the concentrations of main products are affected by the content of hexyl branches in the P-TREF fractions. Also the T_{max} has been obtained as temperature in which most number of products is produced. Moreover, it was found that the temperature can affect the concentrations of pyrolysis products.

ACKNOLEDGMENTS

We thank Kerstin Arnhold and Christina Harnisch from Leibniz-Institut für Polymerforschung (IPF) Dresden e.V. (Germany) for pyrolysis-GC-MS measurements. We are also grateful to Dr. Mikhail Malanin (IPF) for FTIR and Petra Treppe and Dr. Albena Lederer from IPF for SEC-MALLS measurement and discussion, respectively.

REFERENCES

1. Papageorgiou DG, Bikiaris DN, Chrissafis K (2012) Effect of crystalline structure of

polypropylene random copolymers on mechanical properties and thermal degradation kinetics. Thermochimica Acta 543: 288-294
2. Pourtaghi-Zahed H, Zohuri GH (2012) Synthesis and characterization of ethylene-propylene copolymer and polyethylene using α-diimine nickel catalysts. J Polym Res 19: 1-8
3. Mirabella FM, Crist B (2004) Melting behavior of polyethylene/α-olefin copolymers: Narrow composition distribution copolymers and fractions from Ziegler–Natta and single-site catalyst products. J Polym Sci Pol Phys 42: 3416-3427
4. Liu Z, Chen S, Zhang J (2011) Preparation and characterization of ethylene-butene copolymer (EBC)/mica composites. J Polym Res 18: 2403-2413
5. Zhang X-b, Li Z-s, Lu Z-y, Sun C-C (2002) Roles of branch content and branch length in copolyethylene crystallization: Molecular dynamics simulations. Macromolecules 35: 106-111
6. Mauler RS, Galland GB, Scipioni RB, Quijada R (1996) The effect of the ethylene pressure on its reaction with 1-hexene, 1-octene and 4-methyl-1-pentene. Polym Bull 37: 469-474
7. Gomari S, Ghasemi I, Karrabi M, Azizi H (2011) Organoclay localization in polyamide 6/ethylene-butene copolymer grafted maleic anhydride blends: the effect of different types of organoclay. J Polym Res 19: 1-11
8. Pourtaghi-Zahed H, Zohuri GH, Ahmadjo S (2014) Unique microstructure analysis of ethylene-propylene copolymer synthesized using catalytic system based on α-diimine nickel complexes: a comparative study by ^{13}C NMR technique. J Polym Res 21: 1-10
9. Bensason S, Stepanov E, Chum S, Hiltner A, Baer E (1997) Deformation of elastomeric ethylene-octene copolymers. Macromolecules 30: 2436-2444
10. Rabiej S, Goderis B, Janicki J, Mathot V, Koch M, Groeninckx G, Reynaers H, Gelan J, Włochowicz A (2004) Characterization of the dual crystal population in an isothermally crystallized homogeneous ethylene-1-octene copolymer. Polymer 45: 8761-8778
11. Babu RR, Singha NK, Naskar K (2010) Effects of mixing sequence on peroxide cured polypropylene (PP)/ethylene octene copolymer (EOC) thermoplastic vulcanizates (TPVs). Part. II. Viscoelastic characteristics. J Polym Res 18: 31-39
12. Sehanobish K, Patel R, Croft B, Chum S, Kao C (1994) Effect of chain microstructure on modulus of ethylene–α-olefin copolymers. J Appl polym Sci 51: 887-894
13. Bensason S, Minick J, Moet A, Chum S, Hiltner A, Baer E (1996) Classification of homogeneous ethylene-octene copolymers based on comonomer content. J Polym Sci Pol Phys 34: 1301-1315
14. Brady JM, Thomas EL (1988) Effect of short-chain branching on the morphology of LLDPE-oriented thin films. J Polym Sci Pol Phys 26: 2385-2398
15. Mileva D, Zia Q, Androsch R (2010) Tensile properties of random copolymers of propylene with ethylene and 1-butene: Effect of crystallinity and crystal habit. Polym Bull 65: 623-634
16. Galland GB, Mauler RS, de Menezes SC, Quijada R (1995) ^{13}C-NMR study of ethylene/1-hexene and ethylene/1-octene copolymers obtained using homogeneous catalysts. Poly Bull 34: 599-604
17. Koivumäki J (1996) Properties of ethylene/1-octene, 1-tetradecene and 1-octadecene copolymers obtained with Cp_2ZrCl_2/MAO catalyst: Effect of composition and comonomer chain length. Polym Bull 36: 7-12
18. Guo N, Li L, Marks TJ (2004) Bimetallic catalysis for styrene homopolymerization and ethylene-styrene copolymerization. Exceptional comonomer selectivity and insertion regiochemistry. J Am Chem Soc 126: 6542-6543
19. Mileva D, Androsch R, Radusch H-J (2009) Effect of structure on light transmission in isotactic polypropylene and random propylene-1-butene copolymers. Polym Bull 62: 561-571
20. Vanden Eynde S, Mathot V, Höhne G, Schawe J, Reynaers H (2000) Thermal behaviour of homogeneous ethylene-1-octene copolymers and

linear polyethylene at high pressures. Polymer 41: 3411-3423
21. Starck P, Rajanen K, Löfgren B (2002) Comparative studies of ethylene–α-olefin copolymers by thermal fractionations and temperature-dependent crystallinity measurements. Thermochim Acta 395: 169-181
22. Mileva D, Androsch R, Radusch H-J (2008) Effect of cooling rate on melt-crystallization of random propylene-ethylene and propylene-1-butene copolymers. Polym Bull 61: 643-654
23. Alamo RG, Mandelkern L (1994) The crystallization behavior of random copolymers of ethylene. Thermochim Acta 238: 155-201
24. Abbas-Abadi MS, Nekoomanesh N.M, Yeganeh H, Bozorgi B (2013) The effect of melt flow index, melt flow rate, and particle size on the thermal degradation of commercial high density polyethylene powder. J Therm Anal Calorim 114: 1333-1339
25. Kebritchi A, Nekoomanesh M, Mohammadi F, Khonakdar HA (2015) The interrelationships between microstructure and melting, crystallization and thermal degradation behaviors of fractionated ethylene/1-butene copolymer. Iran Polym J 24: 267-277
26. Kebritchi A, Nekoomansh M, Mohammadi F, Khonakdar HA (2015) The ablative behavior of high linear chains and its role in the thermal stability of polyethylene: A combined P-TREF−TGA study. Polym Int 64: 1316-1325
27. Kebritchi A, Nekoomansh M, Mohammadi F, Khonakdar HA (2014) The role of 1-hexene comonomer content in thermal behavior of medium density polyethylene (MDPE) synthesized using Phillips catalyst. Polyolefins J 1: 117-129
28. Kebritchi A, Nekoomanesh H. M, Mohammadi F, Khonakdar HA (2017) Effect of Microstructure of high density polyethylene on catalytic degradation: A comparison between nano clay and FCC. J Polym Environ 21: 1-10
29. Cheruthazhekatt S, Pijpers TF, Mathot VB, Pasch H (2013) Combination of TREF, high-temperature HPLC, FTIR and HPer DSC for the comprehensive analysis of complex polypropylene copolymers. Anal Bioanal Chem 405: 8995-9007
30. Assumption H, Vermeulen J, Jarrett WL, Mathias LJ, Van Reenen A (2006) High resolution solution and solid state NMR characterization of ethylene/1-butene and ethylene/1-hexene copolymers fractionated by preparative temperature rising elution fractionation. Polymer 47: 67-74
31. Müller A, Hernandez Z, Arnal M, Sánchez J (1997) Successive self-nucleation/annealing (SSA): A novel technique to study molecular segregation during crystallization. Polymer Bull 39: 465-472
32. Joe D, Golling FE, Friedemann K, Crespy D, Klapper M, Müllen K (2014) Anisotropic Supports in Metallocene-Catalyzed Polymerizations: Templates to Obtain Polyolefin Fibers. Macromol Mater Eng 299: 1155-1165
33. Dorresteijn R, Nietzel S, Joe D, Gerkmann Y, Fink G, Klapper M, Müllen K (2014) Metallocene supported on porous and nonporous polyurethane particles for ethylene polymerization. J Polym Sci Pol Chem 52: 450-459
34. De Rosa C, Auriemma F, Villani M, Ruiz de Ballesteros O, Di Girolamo R, Tarallo O, Malafronte A (2014) Mechanical Properties and Stress-Induced Phase Transformations of Metallocene Isotactic Poly (1-butene): The Influence of Stereodefects. Macromolecules: 47: 1053-1064
35. Zhang M, Wanke SE (2003) Quantitative determination of short-chain branching content and distribution in commercial polyethylenes by thermally fractionated differential scanning calorimetry. Polym Eng Sci 43: 1878-1888
36. Kakugo M, Miyatake T, Mizunuma K (1991) Chemical composition distribution of ethylene-1-hexene copolymer prepared with titanium trichloride-diethylaluminum chloride catalyst. Macromolecules 24: 1469-1472
37. Adisson E, Ribeiro M, Deffieux A, Fontanille M (1992) Evaluation of the heterogeneity in linear low-density polyethylene comonomer unit distribution by differential scanning calorimetry characterization of thermally treated samples.

Polymer 33: 4337-4342
38. Hosoda S (1988) Structural distribution of linear low-density polyethylenes. Polym J 20: 383-397
39. Mortazavi SMM, Arabi H, Zohuri G, Ahmadjo S, Nekoomanesh M, Ahmadi M (2010) Copolymerization of ethylene/α-olefins using bis (2-phenylindenyl) zirconium dichloride metallocene catalyst: Structural study of comonomer distribution. Polym Int 59: 1258-1265
40. Hosoda S, Nozue Y, Kawashima Y, Suita K, Seno S, Nagamatsu T, Wagener KB, Inci B, Zuluaga F, Rojas G (2010) Effect of the sequence length distribution on the lamellar crystal thickness and thickness distribution of polyethylene: Perfectly equisequential ADMET polyethylene vs ethylene/α-olefin copolymer. Macromolecules 44: 313-319
41. Gauthier E, Laycock B, Cuoq F-M, Halley P, George K (2013) Correlation between chain microstructural changes and embrittlement of LLDPE-based films during photo-and thermo-oxidative degradation. Polym Degrad Stabil 98: 425-435
42. Wilfong DL,Knight G (1990) Crystallization mechanisms for LLDPE and its fractions. J Polym Sci Pol Phys 28: 861-870
43. Zhang M, Lynch D, Wanke S (2001) Effect of molecular structure distribution on melting and crystallization behavior of 1-butene/ethylene copolymers. Polymer 42: 3067-3075
44. Hosoda S, Kojima K, Furuta M (1986) Morphological study of melt-crystallized linear low-density polyethylene by transmission electron microscopy. Die Makromol Chem 187: 1501-1514
45. Kebritchi A, Nekoomanesh H. M, Mohammadi F, Khonakdar HA (2014) The role of 1-hexene comonomer content in thermal behavior of medium density polyethylene (MDPE) synthesized using Phillips catalyst. Polyolefins J 2: 117-129
46. Pielichowski K, Njuguna J (2005) Thermal degradation of polymeric materials. Rapra Technology, Show bury, UK
47. Katritzky AR, Kuanar M, Slavov S, Hall CD, Karelson M, Kahn I, Dobchev DA (2010) Quantitative correlation of physical and chemical properties with chemical structure: Utility for prediction. Chem Rev 110: 5714-5789
48. Lattimer RP (1995) Pyrolysis field ionization mass spectrometry of polyolefins. J Anal Appl Pyrolys 31: 203-225
49. Mastral F, Esperanza E, Berrueco C, Juste M, Ceamanos J (2003) Fluidized bed thermal degradation products of HDPE in an inert atmosphere and in air–nitrogen mixtures. J Anal Appl Pyrolys 70: 1-17
50. Poutsma ML (1990) Free-radical thermolysis and hydrogenolysis of model hydrocarbons relevant to processing of coal. Energy Fuels 4: 113-131
51. Kossiakoff A, Rice FO (1943) Thermal decomposition of hydrocarbons, resonance stabilization and isomerization of free radicals1. J Am Chem Soc 65: 590-595